

Individualized Gait Pattern Generation for Sharing Lower Limb Exoskeleton Robot

Xinyu Wu¹, Member, IEEE, Du-Xin Liu, Student Member, IEEE,
Ming Liu, Member, IEEE, Chunjie Chen, and Huiwen Guo

Abstract—The development of sharing technology makes it possible for expensive lower limb exoskeleton robots to be extensively employed. However, due to the uniqueness of gait pattern, it is challenging for lower limb exoskeleton robot to adapt to different wearers' gait patterns. Studies have shown that the gait pattern is affected by many physical factors. This paper proposes an individualized gait pattern generation (IGPG) method for sharing lower limb exoskeleton (SLEX) robot. First, the gait sequences are parameterized to extract gait features. Then, the Gaussian process regression with automatic relevance determination is used to establish the mapping relationships between the body parameters and the gait features, and the weights of each body parameters on gait pattern are also given. The gait features of an unknown subject can be predicted based on the training set. Finally, the individualized gait pattern is reconstructed by autoencoder neural network and scaling process based on predicted gait features. The experimental results show that the gait pattern predicted by IGPG is very similar to the subject's actual trajectory and has been successfully applied on the SLEX robot. With the help of sharing technology, the training set will be increased, and the prediction accuracy of individualized gait pattern will also be improved.

Note to Practitioners—The main purpose of this paper is to solve the gait pattern mismatch problem when different people wear an lower limb exoskeleton robot. The gait patterns are different for each individual, and the main gait-related factors include body parameters and walking speed (WS). Therefore, the suitable gait pattern for the wearer is predicted according to their body parameters and target WS in this paper. The detailed prediction process and a full analysis of experimental results are

also given. Finally, the generated gait patterns are successfully verified on the lower limb exoskeleton robot.

Index Terms—Gait pattern generation, lower limb exoskeleton robot.

I. INTRODUCTION

ROBOTIC exoskeletons are extensively used in rehabilitation training and walking assisted for those with spinal cord and stroke injuries [1], [2]. Significant achievements have been made in the development of prototypes in recent years, such as LOPES [3], Lokomat [4], ALEX [5], MIND-WALKER [6], and so on [7]. Meanwhile, there are some mature products, such as Ekso [8], ReWalk [9], HAL [10], Indego [11], and REX [12], which have been pushed to the market. However, the price of these products is quite high, making it hard for average families in demands to afford them.

Recently, the sharing economy has gained recognition and support. It is known as collaborative consumption that people share the services rather than having individual ownership [13], [14]. The sharing application can reduce the consumption cost for users and improve the product utilization [15]–[18]. In fact, expensive lower limb exoskeleton robots that are mainly used for rehabilitation training and assist people walking are suitable for sharing applications, which can benefit more patients with spinal cord and stroke injuries. The reasons for this can be summarized as follows: 1) there are many patients with hemiplegia, paraplegia, stroke, spinal cord injury, and so on. Robotic gait training through walking can help patients to prevent the muscle atrophy and promote the body metabolism. There is an enormous potential market demand; 2) the price of existing lower limb exoskeleton robots is quite high that many ordinary families can hardly afford them; and 3) at present, the Internet-based technology for sharing economy has been well developed, such as sharing bicycles (Mobike, China), for-profit service provision (Uber, U.S.), rental (Airbnb, U.S.), and gifting (Freecycle, U.S.) platform. Therefore, it is feasible to share the lower limb exoskeleton robots, so that the patients would only need to buy the required services from exoskeleton robots.

The primary function of lower limb exoskeleton robots for rehabilitation is to assist patients in walking [19]. The main technical points include motion intention recognition, gait pattern generation, and stable gait control [20]–[22]. The existing research results show that each person's gait pattern is unique [23]. Accordingly, it is necessary for the robot to automatically adapt to various gait patterns while shared by different patients. The previous studies have shown that the

Manuscript received October 13, 2017; revised April 8, 2018; accepted May 15, 2018. This paper was recommended for publication by Associate Editor X. Li and Editor M. P. Fantl upon evaluation of the reviewers' comments. This work was supported in part by the NSFC-Shenzhen Robotics Research Center Project under Grant U1613219, in part by the National Basic Research Program (973 Program) under Grant 2015CB351706, and in part by the Shenzhen Fundamental Research and Discipline Layout project under Grant JCYJ20150925163244742. (Corresponding author: Xinyu Wu.)

X. Wu is with the CAS Key Laboratory of Human-Machine Intelligence-Synergy Systems, Shenzhen Institutes of Advanced Technology, Chinese Academy of Sciences, Shenzhen 518055, China, and also with the Department of Mechanical and Automation Engineering, The Chinese University of Hong Kong, Hong Kong (e-mail: xy.wu@siat.ac.cn).

D.-X. Liu and C. Chen are with the CAS Key Laboratory of Human-Machine Intelligence-Synergy Systems, Shenzhen Institutes of Advanced Technology, Chinese Academy of Sciences, Shenzhen 518055, China, and also with the Shenzhen College of Advanced Technology, University of Chinese Academy of Sciences, Beijing 100049, China.

M. Liu is with the Department of Electronics and Computer Engineering, Hong Kong University of Science and Technology, Hong Kong.

H. Guo is with the CAS Key Laboratory of Human-Machine Intelligence-Synergy Systems, Shenzhen Institutes of Advanced Technology, Chinese Academy of Sciences, Shenzhen 518055, China.

Color versions of one or more of the figures in this paper are available online at <http://ieeexplore.ieee.org>.

Digital Object Identifier 10.1109/TASE.2018.2841358

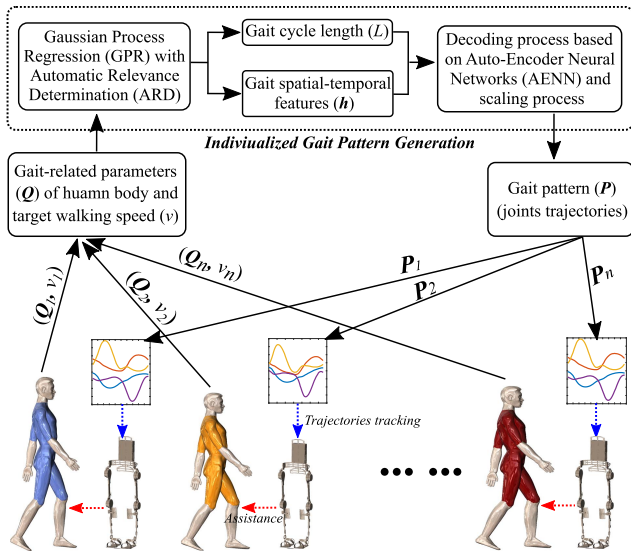


Fig. 1. Framework of IGPG. A suitable gait pattern can be predicted by the IGPG method according to given body parameters and target WS.

walking gait pattern is related to walking speed (WS), gender, age, other human body parameters, and also the emotional states [24], [25], [41]. In order to find out the body parameters that affect the gait pattern as comprehensively as possible, this paper measures as many body parameters as possible according to the existing research results.

The focus of this paper is to build an individualized gait pattern generation (IGPG) model, which can describe the relationships between human body parameters and gait patterns with different WSs based on acquired gait data. Thus, while entering a new subject's body parameters and a target WS, the model can give an individualized gait pattern for subject's body characteristics (see Fig. 1). First, the gait features including gait cycle length (GCL) and gait spatial-temporal (GST) features are extracted. The GST features are obtained by the encoding process of the autoencoder neural network (AENN) [27]. Then, the mapping relationships between the body parameters and gait features at different WSs are established by Gaussian process regression (GPR) with automatic relevance determination (ARD) [28]. Thus, while given new body parameters and target WS, the model can predict suitable gait features. Finally, the gait pattern can be reconstructed by decoding process of AENN and scaling process based on predicted gait features. By analyzing the error and correlation of the predictive gait pattern and applying them on SLEX robot, the results demonstrate that the proposed method can better generate the individualized gait pattern.

The major contributions of this paper are the following: 1) the proposed IGPG model can predict a suitable gait pattern, which can be applied on the lower limb exoskeleton robot according to (21) given body parameters and target WS; 2) a new gait features extraction method based on AENN is proposed; and 3) the affected weights of gait-related body parameters on gait pattern are given based on GPR with ARD.

The rest of this paper is organized as follows. Section II discusses the related work. The notations, assumptions, and problem definition are given in Section III. Section IV presents

the IGPG method. Then, the experimental results and analysis are presented in Section V, and conclude the paper and discuss the future work in Section VI.

II. RELATED WORK

The development of sharing technology improves the utilization of intelligent devices, services, and information, and also reduces the cost of using them. In recent years, the application of sharing technology becomes more and more popular in the field of medical rehabilitation [29]. Kim *et al.* [30] help users to get the proper guidelines or treatments by sharing users' own healthcare data with mobile phone. Chen *et al.* [31] propose a cloud-computing-based rehabilitation services system to solve the difficulties of data sharing and mass data processing.

Aiming at the patients with lower limb disabilities, the lower limb exoskeleton robots are employed to assist them to walk automatically. Because their lower limbs have lost the capacities of motion, they cannot rely on their strength, muscles, and so on. to guide the exoskeleton robot movement. Therefore, the predefined gait trajectory control strategies are usually adopted to help these patients walk [21]. Initially, the predefined gait trajectory is prerecorded from a healthy person or obtained from clinical gait database. Merodio *et al.* [32] employ two finite-state machines to separately adjust the hip and knee joints trajectories recorded from healthy children for ATLAS robot. Suzuki *et al.* [33] use a real-time intention estimator to control the desired joints patterns which are recorded from a healthy subject. These gait patterns are too stiff.

How to plan an appropriate gait pattern for each patient has become a hot topic of lower limb exoskeleton robot research. Considering the sharing application of robot, the problem becomes more serious. The methods of gait pattern generation have been utilized on exoskeleton robot. For example, Vallery *et al.* [34] propose an online trajectory generation method called complementary limb motion estimation that can be applied to hemiplegic subjects. Kagawa *et al.* [35] propose a motion planning method in joint space for a wearable robot with a variable stride length and WS, which considered the thigh and shank cuffs and the position of the joint. However, these methods are only taking legs symmetry or leg length into account when predicting the gait pattern. Karunakaran *et al.* [36] propose user control of gait in real time using healthy upper extremities, and the importance of haptics in generating exoskeleton gait trajectory is verified. Zhang *et al.* [37] develop optimized torque patterns for identifying the exoskeleton assistance that minimizes human energy cost during walking to satisfy the individual needs.

Early medical studies showed that if all the measurements are considered, the gait is unique [23], and each person has a distinctive and idiosyncratic way of walking [26]. In fact, there are many factors affecting the gait pattern, such as walkers' age, height, weight, leg length, and mood. In natural and individual-specific gait planning, Low *et al.* [38]–[40] have made a great improvement. In [38], according to age, gender, body height (BH), and body weight of target subject,

a multilayer perceptron neural network is used to predict the corresponding natural gait parameters, such as cadence, stride length, and WS. In [39], a natural and tunable rehabilitation gait system is developed, and the body parameters, such as thigh length (TL), calf length, and the length between ankle joint to metatarsal, are taken into account in a subject-based motion generation model. In [40], an individual-specific gait pattern prediction model (GPPD) is proposed based on generalized regression neural networks, and the lower limb joint angle waveforms can be predicted by the model according to target gait parameters, such as stride length and cadence and body parameters such as Anterior Superior Iliac Spine breadth, TL, calf length, and foot length (FL). Yun *et al.* [41] select several body parameters that significantly affect the gait pattern to predict gait kinematics of single WS by GPR. However, these methods are not comprehensive enough to take into account the physical parameters that affect the gait pattern or cannot generate different gait patterns with WS changing.

Several lower limb exoskeleton robots for rehabilitation walking have been developed in the previous work. Based on the robots, some research on optimal gait planning has been performed. In [42], the stroke patients are provided with a more convenient, cost-effective, and personalized physical rehabilitation training by using the virtual reality technology. It can create various training plans for different patients and guide the patients how to complete the training plan. In [43], the recurrent neural network with long–short-term memory units is adopted to generate an optimal trajectory of an abnormal knee based on other normal joints' data. To generate suitable joint trajectory for the wearer, the neural network is trained by large amount of gait data from different subjects, so that the spatial–temporal features of the gait can be obtained as many as possible. However, this learning-based approach does not take into account the body parameters that affect either of the gait patterns. To investigate an individualized gait pattern, a new exoskeleton robot for rehabilitation walking named sharing lower limb exoskeleton (SLEX) is developed recently. The method of this paper will be verified on SLEX.

III. PROBLEM DEFINITION

The goal of this paper is to obtain an individualized walking gait of the subject according to their body parameters and target WS, so that the SLEX robot can assist the subject in walking. Considering the characteristics of walking gait and the feasibility of sampling, three assumptions are made as follows.

- 1) Because of great differences between different walking modes, only level-ground walking in a straight line is considered here.
- 2) The subjects and SLEX robot can maintain balance by upper limbs and handrails which do not affect the walking gait pattern.
- 3) Since the gait pattern is periodic, the object of this paper is a single “gait cycle.”

The notations of variables are defined as follows:

- lh left hip joint;
- lk left knee joint;
- rh right hip joint;
- rk right knee joint;
- v walking speed, $v \in \{1.5, 2, 2.5, 3, 3.5, 4, 4.5\}$, unit: km/h;
- L GCL);
- \mathbf{h} gait spatial-temporal (GST) features;
- θ_j angular trajectory sequence of j th lower limb joint in sagittal plane with length N , $j \in \{lh, lk, rh, rk\}$
- \mathbf{Q}_i observable variable, D -dimensional body parameters of i th subject, $\mathbf{Q}_i \in \mathbb{R}^D$;
- \mathbf{P}_i observable variable, walking gait trajectory representing gait pattern of i th subject during one gait cycle, $\mathbf{P}_i = [\theta_{lh}, \theta_{lk}, \theta_{rh}, \theta_{rk}]^T$;
- \mathbf{H}_i d -dimensional gait features extracted from \mathbf{P}_i .

The gait related body parameters and abbreviated forms are defined as follows: 1) age (AG); 2) weight (WT); 3) waist circumference (WC); 4) TL; 5) shank length (SL); 6) maximum thigh width (TW); 7) FL; 8) foot breadth (FB); 9) forefoot length (FF); 10) ankle width (AW); 11) ankle circumference; 12) bi-ankle outer width (AO); 13) knee width (KW); 14) knee circumference (KC); 15) bi-knee outer width (KO); 16) bi-hip width (HW); 17) bi-iliac width (IW); 18) BH; 19) hip height (HH); 20) knee height (KH); and 21) ankle height (AH).

In this paper, the walking gait pattern is represented by four angular trajectories of right hip, right knee, left hip, and left knee flexions/extensions in sagittal plane. Seven WSs are also considered. This paper will predict a suitable walking gait pattern for each individual. From [23] and [26], it can be concluded that the gait pattern is associated with body parameters and WS. Therefore, the appropriate sequences of joint trajectories should be predicted through body parameters at a given WS

$$\mathbf{P}_* = \mathcal{G}(\mathbf{Q}_*, v_* | \mathbf{Q}, v, \mathbf{P}) \quad (1)$$

where \mathbf{Q} , v , and \mathbf{P} are from the training gait set, \mathbf{Q}_* and v_* are the body parameters of the new subject and the target WS, and \mathbf{P}_* is the predictive gait pattern. The ultimate goal of this paper is to establish the relationship $\mathcal{G}(\cdot)$, namely, the proposed IGPG method.

IV. INDIVIDUALIZED GAIT PATTERN GENERATION

A. Framework of Individualized Gait Pattern Generation

To generate an individualized gait pattern, 21 physical factors (body parameters) and a WS that may affect gait pattern are considered. The IGPG includes three processes, as presented in Fig. 2. The input includes new body parameters and target WS, and the output is the individualized gait pattern. During the method, the encoding process of AENN is employed for extracting the GST features, while the decoding process is employed for reconstructing the gait pattern. The resampling method is adopted to scale the gait sequences.

To better establish the mapping relationships between the body parameters and the gait pattern, the gait features including GCL and GST features are first extracted. Then,

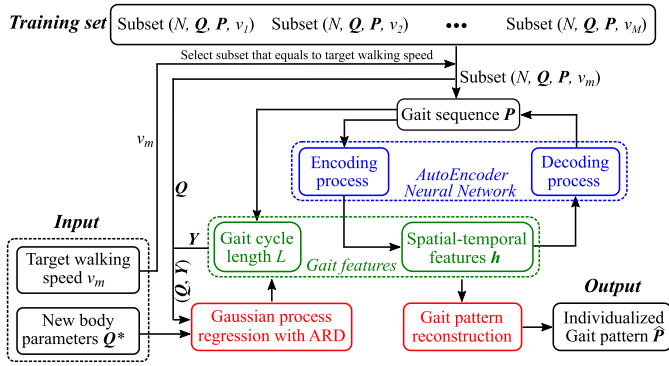


Fig. 2. Framework of IGPG method.

the gait features can be predicted through GPR with ARD based on body parameters. Finally the gait pattern is reconstructed based on predictive gait features.

B. Gait Features Extraction and Gait Pattern Reconstruction

The gait pattern is represented by the rotational trajectories of lower limb joints, and the uniqueness of gait pattern determines the variety of gait features. Therefore, it is difficult to use accurate mathematical functions to represent the variable gait patterns.

To generate an individualized gait pattern, Lim *et al.* [38] take the stride length and cadence as the main features of gait pattern. Trieu *et al.* [40] adopt Fourier coefficient vectors to represent the joint angle waveform by Fourier transform and then reconstruct the joint angle waveform by inverse Fourier transform. Yun *et al.* [41] take the gait period, pelvis position and rotation, and the rotations of the lower limb joints as the gait features to be predicted.

In this paper, since the generated gait patterns are mainly used on the SLEX lower limb exoskeleton robot, the gait pattern \mathbf{P} is represented first by four joint angle sequences

$$\mathbf{P} = \begin{bmatrix} \theta_{lh} \\ \theta_{lk} \\ \theta_{rh} \\ \theta_{rk} \end{bmatrix} = \begin{bmatrix} \theta_{lh1} & \theta_{lh2} & \theta_{lh3} & \dots & \theta_{lhL} \\ \theta_{lk1} & \theta_{lk2} & \theta_{lk3} & \dots & \theta_{lkL} \\ \theta_{rh1} & \theta_{rh2} & \theta_{rh3} & \dots & \theta_{rhL} \\ \theta_{rk1} & \theta_{rk2} & \theta_{rk3} & \dots & \theta_{rkL} \end{bmatrix}. \quad (2)$$

It is not feasible to generate variable gait sequences directly according to fixed body parameters. Therefore, the gait sequences should be parameterized, so that the gait pattern can be reconstructed through parametric gait features. Here, the gait features extracted from a single gait cycle of one joint θ_i are classified as two types: scalar *GCL* L and s -dimensional *spatial-temporal features* $\mathbf{h} = [h_1, h_2, \dots, h_s]^T$. For ease of writing, we notate $d = 1 + s$. Therefore, the combined *gait features* $\mathbf{H} = \begin{bmatrix} L \\ \mathbf{h} \end{bmatrix}$, $\mathbf{H} \in \mathbb{R}^d$. First, the length L of the gait cycle θ_i is retained

$$L = \text{length}(\theta_i). \quad (3)$$

Because everyone has a walking pattern that is most natural and comfortable for them, different subjects have different GCLs even at the same WS.

Then, the AENN is adopted to extract the GST features and reconstruct the gait pattern. The gait cycle is resampled to be of fixed length L_0

$$\theta_i = [\theta_1, \theta_2, \dots, \theta_L] \Rightarrow \tilde{\theta}_i = [\tilde{\theta}_1, \tilde{\theta}_2, \dots, \tilde{\theta}_{L_0}] \quad (4)$$

where $\Rightarrow \tilde{\theta}_i$ is the new data of i th joint by resampling.

The AENN has three layers: input layer, hidden layer, and output layer. The number of hidden layer neurons is s , namely, the dimension of GST features is s . Functionally, it includes two parts: *encoding process* and *decoding process*.

The GST features extraction (namely *encoding process*) is

$$\mathbf{h} = \mathbf{W}_{\text{en}} \tilde{\theta}_i + \mathbf{b}_{\text{en}} \quad (5)$$

where \mathbf{W}_{en} is a $s \times L_0$ encoding weight matrix, \mathbf{b}_{en} is a $s \times 1$ encoding bias vector, and \mathbf{h}_i are low-dimensional $s \times 1$ gait features that are extracted from $\tilde{\theta}_i$.

The gait pattern reconstruction includes *decoding process* and *scaling process*. The decoding process is

$$\hat{\theta}_i = \mathbf{W}_{\text{de}} \mathbf{h} + \mathbf{b}_{\text{de}} \quad (6)$$

where \mathbf{W}_{de} is a $L_0 \times s$ decoding weight matrix, \mathbf{b}_{de} is a $L_0 \times 1$ decoding bias vector, and $\hat{\theta}_i$ is the reconstructed fixed-length gait sequence based on GST features \mathbf{h} .

The AENN is trained with a large number of gait data, so that it can obtain the main features of gait sequences. During training, the outputs of network keep approximating inputs by minimizing the error between $\hat{\theta}_i$ and θ_i . The root-mean-square error (RMSE) method is used to evaluate the performance of trained AENN

$$e_{\text{RMSE}} = \sqrt{\frac{\|\hat{\theta}_i - \theta_i\|}{L_0}}. \quad (7)$$

The scaling process is also a resampling process from L_0 points to L points

$$\begin{aligned} \hat{\theta}_i &= [\hat{\theta}_1, \hat{\theta}_2, \dots, \hat{\theta}_{L_0}] \\ \Rightarrow \theta_i^* &= [\theta_1^*, \theta_2^*, \dots, \theta_L^*]. \end{aligned} \quad (8)$$

Therefore, the model has the abilities of automatic extraction of gait features, and gait pattern reconstruction based on gait features. By the above-mentioned processes, the gait features extraction and the gait pattern reconstruction for four lower limb joints during one walking cycle can be achieved.

C. Gaussian Process for Gait Features Regression

Based on Sections IV-A and IV-B, two types of gait features can be obtained: the scalar GCL L and s -dimensional gait features vector \mathbf{h} extracted from the L_0 -dimensional gait sequence θ_i . With these s gait features, the target gait sequences of lower limb joints can be reconstructed.

By analyzing the collected gait set and extracted gait features, it can be seen that the body parameters and gait features of a gait set approximately obey Gaussian distributions. Here the body parameters $\mathbf{Q} \in \mathbb{R}^{N \times D}$ are D dimensions, and N is the number of subjects in training set

$$\mathbf{Q} = \begin{bmatrix} \mathbf{Q}_1 \\ \mathbf{Q}_2 \\ \dots \\ \mathbf{Q}_N \end{bmatrix} = \begin{bmatrix} Q_{11} & Q_{12} & Q_{13} & \dots & Q_{1D} \\ Q_{21} & Q_{22} & Q_{23} & \dots & Q_{2D} \\ \dots & \dots & \dots & \dots & \dots \\ Q_{N1} & Q_{N2} & Q_{N3} & \dots & Q_{ND} \end{bmatrix}. \quad (9)$$

Assuming that the gait pattern at WS v is denoted as \mathbf{P}_v , the gait features extracted from gait pattern \mathbf{P}_v are denoted as $\mathbf{Y}_v \in \mathbb{R}^{N \times d}$

$$\mathbf{Y}_v = \begin{bmatrix} \mathbf{H}_1^T \\ \mathbf{H}_2^T \\ \dots \\ \mathbf{H}_N^T \end{bmatrix} = \begin{bmatrix} L_1 & h_{11} & h_{12} & \dots & h_{1s} \\ L_2 & h_{21} & h_{22} & \dots & h_{2s} \\ \dots & \dots & \dots & \dots & \dots \\ L_N & h_{N1} & h_{N2} & \dots & h_{Ns} \end{bmatrix}. \quad (10)$$

The goal of this paper is to obtain the mapping relationship between each gait feature and all body parameters \mathbf{Q} at a given WS v . As a result, when new body parameters are given, the gait features at a given WS can be predicted. To facilitate the calculation, each time one gait feature of \mathbf{H} is predicted by GPR. 1-D feature during \mathbf{Y}_v is marked as $\mathbf{Y}_{:,i|v}$. For brevity

$$\mathbf{y} = \mathbf{Y}_{:,i|v}. \quad (11)$$

Therefore, each gait feature \mathbf{y} can be thought of as being related to an underlying function $f(\cdot)$ through a Gaussian noise model

$$\mathbf{y} = f(\mathbf{Q}) + \boldsymbol{\epsilon} \quad (12)$$

where $\boldsymbol{\epsilon} = [\epsilon_1, \epsilon_2, \dots, \epsilon_N]^T$ is an independent identically distributed Gaussian noise with mean 0 and variance σ_n^2 . The functional collection $[y_1, y_2, \dots, y_N]^T$ follows the multivariate Gaussian distribution:

$$[y_1, y_2, \dots, y_N]^T \sim \mathcal{N}(\boldsymbol{\mu}, \mathbf{K}) \quad (13)$$

where $\boldsymbol{\mu} = \mathbf{0}$ is the mean vector and \mathbf{K} is the $N \times N$ covariance matrix of which the (i, j) th element $K_{ij} = \kappa(\mathbf{Q}_i, \mathbf{Q}_j)$.

From [23], [26], [40], and [41], different body parameters have different influences on the walking gait pattern. In order to better establish the relationship between the body parameters and gait features, the effects of different dimensional body parameters on walking gait pattern need to be quantified. In [44], to determine a value for the correlation length scale in a Gaussian process, a separate parameter for each input variable is incorporated. Such a covariance function that implements ARD is presented in [28]. Therefore, the kernel function with ARD is selected to automatically determine which body parameters are more relevant

$$\kappa(\mathbf{Q}_i, \mathbf{Q}_j) = \sigma_f^2 \exp\left(-\frac{1}{2} \sum_{k=1}^D \eta_k (\|\mathbf{Q}_{ik} - \mathbf{Q}_{jk}\|^2)\right) + \sigma_n^2 \delta(\mathbf{Q}_i, \mathbf{Q}_j) \quad (14)$$

where the maximum allowable covariance is defined as σ_f^2 , η_k is a precision parameter corresponding to the k th body parameter, σ_n^2 is the Gaussian noise defined earlier, and $\delta(\mathbf{Q}_i, \mathbf{Q}_j)$ is the Kronecker delta function. These precision parameters $[\eta_1, \eta_2, \dots, \eta_D]$ can be adapted to a gait set by using maximum likelihood. The larger the parameter η_k , the greater effect of k th body parameter \mathbf{Q}_k on the function; the smaller the parameter η_k , the less the effect of corresponding body parameter.

When given a new subject with body parameters \mathbf{Q}_* , the joint distribution of training gait feature \mathbf{y} and predictive

gait feature y_* are given as

$$\begin{bmatrix} \mathbf{y} \\ y_* \end{bmatrix} \sim \mathcal{N}\left(\begin{bmatrix} \mathbf{0} \\ \mathbf{0} \end{bmatrix}, \begin{bmatrix} \mathbf{K} & K(\mathbf{Q}, \mathbf{Q}_*) \\ K(\mathbf{Q}_*, \mathbf{Q}) & K(\mathbf{Q}_*, \mathbf{Q}_*) \end{bmatrix}\right) \quad (15)$$

where $K(\mathbf{Q}_*, \mathbf{Q}) = [\kappa(\mathbf{Q}_*, \mathbf{Q}_1), \kappa(\mathbf{Q}_*, \mathbf{Q}_2), \dots, \kappa(\mathbf{Q}_*, \mathbf{Q}_N)]$, with the symmetry of covariance function, $K(\mathbf{Q}, \mathbf{Q}_*) = K(\mathbf{Q}_*, \mathbf{Q})^T$.

Based on earlier joint probability distribution, the conditional distribution of predictive gait feature y_* for GPR can be obtained

$$y_* | \mathbf{Q}, \mathbf{y}, \mathbf{Q}_* \sim \mathcal{N}(\mu_*, \sigma_*^2) \quad (16)$$

where

$$\begin{aligned} \mu_* &= K(\mathbf{Q}_*, \mathbf{Q}) \mathbf{K}^{-1} \mathbf{y} \\ \sigma_*^2 &= K(\mathbf{Q}_*, \mathbf{Q}_*) - K(\mathbf{Q}_*, \mathbf{Q}) \mathbf{K}^{-1} K(\mathbf{Q}, \mathbf{Q}_*)^T. \end{aligned} \quad (17)$$

So far, the probability distribution of gait feature y_* can be obtained based on given body parameters \mathbf{Q}_* and training gait set (\mathbf{Q}, \mathbf{y}) . The effect of gait feature regression depends on the choice of kernel function. Here, the exponential-quadratic kernel with ARD framework and Gaussian noise term is selected. However, the hyperparameters $\boldsymbol{\beta} = \{\sigma_f, \eta_1, \eta_2, \dots, \eta_D, \sigma_n\}$ in covariance function are also need to be chosen sensibly. In fact, the maximum posteriori estimate of $\boldsymbol{\beta}$ occurs when $p(\boldsymbol{\beta} | \mathbf{Q}, \mathbf{y})$ at its greatest. According to Bayes' theorem, assuming there is little prior knowledge about what $\boldsymbol{\beta}$ should be during training set, this corresponds to maximizing likelihood function $p(\mathbf{y} | \mathbf{Q}, \boldsymbol{\beta})$ given as

$$p(\mathbf{y} | \mathbf{Q}, \boldsymbol{\beta}) = \frac{1}{(2\pi)^{\frac{N}{2}} |\mathbf{K}|^{\frac{1}{2}}} \exp\left(-\frac{1}{2} \mathbf{y}^T \mathbf{K}^{-1} \mathbf{y}\right). \quad (18)$$

In order to facilitate the calculation, the logarithm is taken on formula (18)

$$\log p(\mathbf{y} | \mathbf{Q}, \boldsymbol{\beta}) = -\frac{N}{2} \log 2\pi - \frac{1}{2} \log |\mathbf{K}| - \frac{1}{2} \mathbf{y}^T \mathbf{K}^{-1} \mathbf{y}. \quad (19)$$

For nonlinear optimization, the conjugate gradients algorithm is adopted to maximize the log-likelihood function with respect to hyperparameter vector $\boldsymbol{\beta}$. With the nonconvex function of $\log p(\mathbf{y} | \mathbf{Q}, \boldsymbol{\beta})$, the choices of initial values of hyperparameters $\boldsymbol{\beta}$ will affect the outcome of regression.

D. Evaluation Criteria of Model Performance

The IGPG performance is mainly evaluated by whether the generated gait sequence is consistent with the subject's own real gait sequence. Because the GCL is one of the main features of gait pattern, it is difficult to accurately evaluate the model when GCLs are inconsistent. Therefore, a two-step evaluation of the predictive GCL and reconstructed fixed-length gait sequence is performed, respectively.

GCL is a scalar. In a gait set, the gait lengths of samples are the real walking results, so it has a high credibility. The maximum L_{\max} and the minimum L_{\min} values are taken as the range of GCL of subject. The GCL mean is $L = (L_{\max} + L_{\min})/2$. The deviation error (DE) is as a measure of prediction accuracy

$$\delta_{\text{DE}} = \frac{L' - L}{L} * 100\%. \quad (20)$$

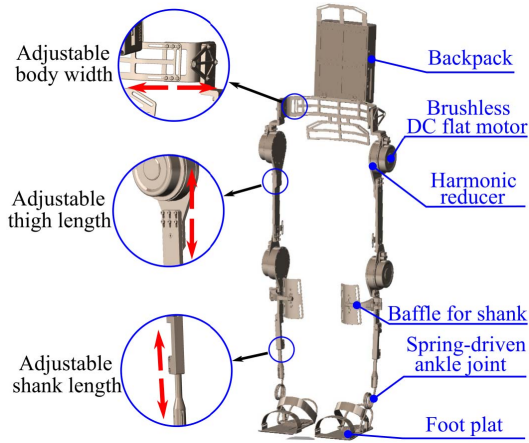


Fig. 3. SLEX robot system.

The correlation coefficient ρ and mean absolute deviation (MAD) are used to evaluate the reconstructed gait sequence. The real walking gait sequence after scaling is notated as $\tilde{\theta}$ and the reconstructed gait sequence before scaling is notated as $\hat{\theta}$ which are equal length sequences. Therefore, the correlation coefficient is

$$\rho = \frac{\text{cov}(\tilde{\theta}, \hat{\theta})}{\sqrt{\text{var}(\tilde{\theta})\text{var}(\hat{\theta})}} \quad (21)$$

and the MAD is

$$\text{MAD} = \sum_{k=1}^{L_0} \frac{|\tilde{\theta}_k - \hat{\theta}_k|}{L_0}. \quad (22)$$

The performance of the IGPG method is evaluated by above-mentioned three indicators.

V. EXPERIMENTS AND ANALYSIS

A. Sharing Lower Limb Exoskeleton Robot

The SLEX lower limb exoskeleton robot has been developed for assisting patients in walking, which can adapt human body sizes for different wearers (Fig. 3). On the joint configuration, the SLEX is approximately consistent with the human lower limb joints. It has hip joints, knee joints, and ankle joints, and the distribution of degrees of freedom. The actuator types are presented in Table I. The hip flexion/extension and knee flexion/extension are driven by brushless dc-flat motors, and the ankle flexion/extension is a spring-driven joint.

B. Data Set for Human Body and Walking Gait

To generate an individualized gait pattern of the wearer for the lower limb exoskeleton robot, 33 subjects are recruited to participate in this experiment and establish the human body and walking gait data set. (approved with IRB No. Shenzhen Institutes of Advanced Technology (SIAT)-IRB-170315-H0142). Each subject is first measured for 21 gait-related body parameters (see Fig. 4). To facilitate the measurement and data collection, only male subjects are recruited in this experiment, so the gait-related body parameters do not include gender. The statistical result of all the subjects' body parameters is given in Table II, including the

TABLE I

DISTRIBUTION OF DEGREES OF FREEDOM AND JOINT ACTUATOR TYPES

Joint	DoFs	Actuator Type
Hip Flexion/Extension	2	Motor-driven
Knee Flexion/Extension	2	Motor-driven
Ankle Flexion/Extension	2	Spring-driven

TABLE II

STATISTICAL RESULT OF BODY PARAMETERS

Body par.	Mean \pm std.	Body par.	Mean \pm std.
AG	25.4 \pm 2.5 (years)	AO	14.6 \pm 0.7 (cm)
WT	66.3 \pm 9.8 (kg)	KW	10.6 \pm 0.8 (cm)
WC	81.8 \pm 7 (cm)	KC	36.8 \pm 2.2 (cm)
TL	38 \pm 2 (cm)	KO	23.5 \pm 2.2 (cm)
SL	41.9 \pm 2.4 (cm)	HW	18.3 \pm 2.3 (cm)
TW	33 \pm 2.1 (cm)	IW	31.6 \pm 2.7 (cm)
FL	25.3 \pm 1.2 (cm)	BH	173 \pm 6.4 (cm)
FB	9.5 \pm 0.7 (cm)	HH	84.4 \pm 4.4 (cm)
FF	6.6 \pm 0.5 (cm)	KH	47.4 \pm 3.2 (cm)
AW	6.9 \pm 0.4 (cm)	AH	6.7 \pm 0.4 (cm)
AC	24.5 \pm 1.3 (cm)		

means and the standard deviations. The target of this paper is to generate individualized gait pattern, and then apply the gait pattern on the lower limb exoskeleton robot. Therefore, only the angular trajectories of hip and knee joints flexion/extension which are motor-driven joints on SLEX are recorded. These subjects are asked to walk on the treadmill in their natural and suitable states during seven different WSs. The lower limb joints trajectories are recorded by the motion capture system of *NoitomTM*. Since the system captures three rotational degrees of freedom per joint, and the rotational angles of the flexion/extension sagittal plane of the SLEX robot need to be controlled, only the angles of hip flexion/extension and knee flexion/extension are kept (see Fig. 4).

The sampling frequency of the capture system is 125 Hz. The seven fixed WSs include: {1.5, 2, 2.5, 3, 3.5, 4, 4.5} km/h. The walking gait data at each WS include about 20 gait cycles.

C. Data Preprocessing

Due to measure errors of sensors, the walking gait data should be filtered first. In [40], the power spectral density analysis was conducted, and the results revealed that over 96.2% of the power of hip and knee joints are contained below 6 Hz. In this paper, a 6-Hz Butterworth low-pass filter is applied on the collected gait data, and the curves of before and after filtering are partially shown in Fig. 5. The raw data and filtered data are represented separately in the form of dotted and solid lines. Obviously, the filtered gait data are smoother than the raw data.

The object of this paper is one gait cycle. Therefore, one gait sequence is divided into several gait cycles during data preprocessing. The maximum angle of the left hip is taken as the cutoff point to divide the gait sequence (see Fig. 5). Then, five stable cycles are selected from the divided gait cycles as the gait patterns of the subject at the current WS.

D. Gait Features Extraction

According to Section IV-B, the gait features' extraction include two steps: GCL extraction and GST features extraction.

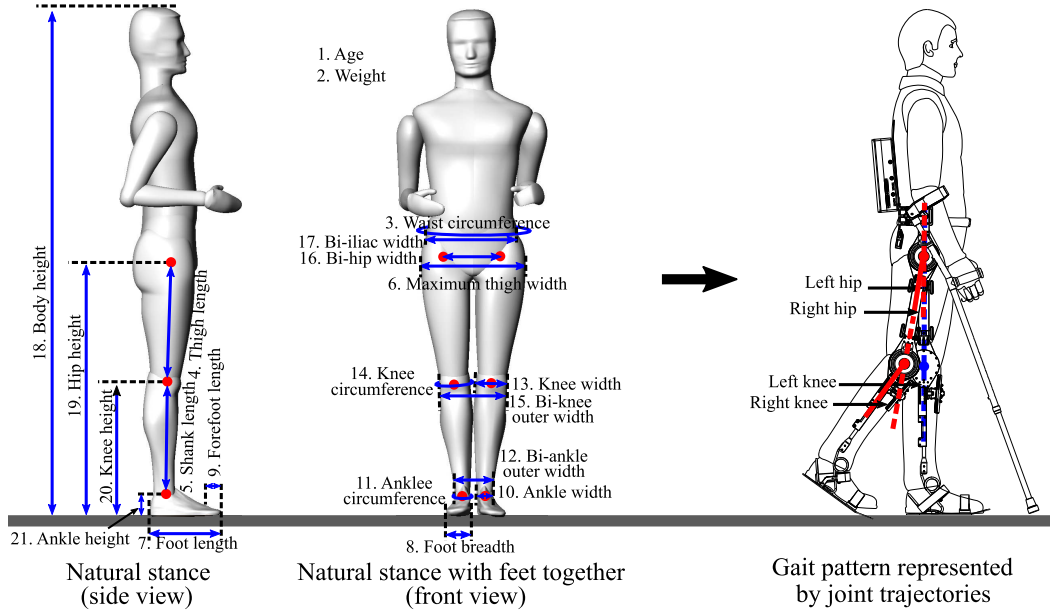


Fig. 4. Gait related body parameters and joint angles representing gait pattern.

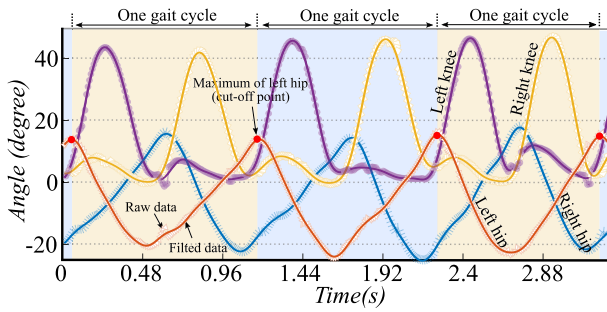


Fig. 5. Gait sequence filtering and gait cycles division.

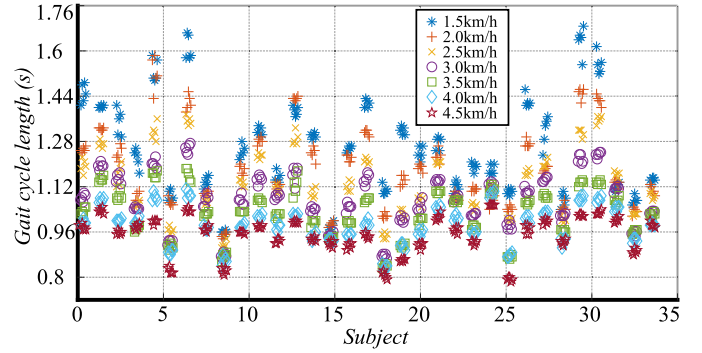


Fig. 6. GCL distribution of subjects during different WSs.

1) *Gait Cycle Length Extraction*: By formula (3), the length of each gait cycle of subjects at different WSs can be obtained, as shown in Fig. 6. The unit of GCL is the sampling point, and the sampling interval is 8 ms.

For different subjects, the range of GCL is different. As shown in Fig. 6, the GCLs of subject #7 vary greatly at different WSs, and the subject #15's vary a little. However, for different WSs, the collected data basically show that the faster the WS, the shorter the GCL; conversely, the smaller the WS, the longer the GCL.

After extracting the feature of GCL, the fixed length of gait cycle L_0 is determined as 150. Accordingly, each gait cycle is resampled to a 4×150 matrix by formula (4). The number of gait cycles for training the AENN is 1155 (33 subjects \times 7 speeds \times 5 cycles).

First of all, it is needed to determine how many dimensions of GST features are most feasible. In order to find out the appropriate s , the AENN is trained with different s based on fixed gait cycles set and the same training epoch. As the dimension s of GST features increases, the changes of RMSE are shown in Fig. 7.

Here, two principles are followed to determine s : 1) the errors of output $\hat{\theta}_i$ and input θ_i are as small as possible and 2) the dimension s of GST features is also as small as possible.

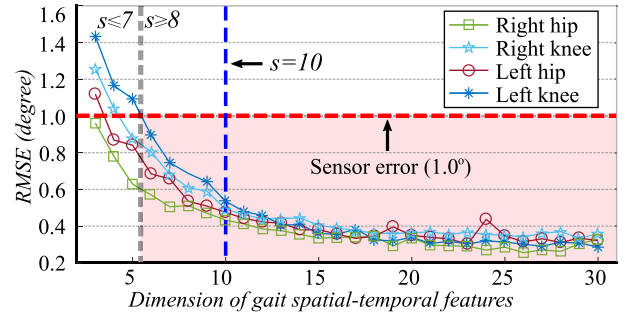


Fig. 7. RSMEs between the input and the output of AENN during different dimensions of GST features.

As shown in Fig. 7, the red dotted line is the sensor error level, and the RMSE of the AENN should be smaller than the sensor error. Accordingly, the dimension s should be larger than 8. For the accuracy of gait features extraction, the dimension of GST features are determined as 10.

2) *Gait Spatial-Temporal Features Extraction*: Through the earlier process, the 10-D GST features for a single joint of each gait cycle can be obtained. During the preprocessing of gait data, five gait cycles for each subject at a fixed WS are selected. These five gait cycles appear in a walking sequence

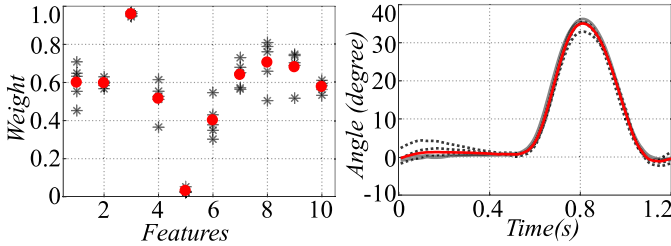


Fig. 8. Averaged GST features and reconstructed gait sequence. Gray stars: GST features (left). Gray lines: original gait sequences (right). Red stars: averaged GST features. Red line: reconstructed gait sequence based on averaged GST features.

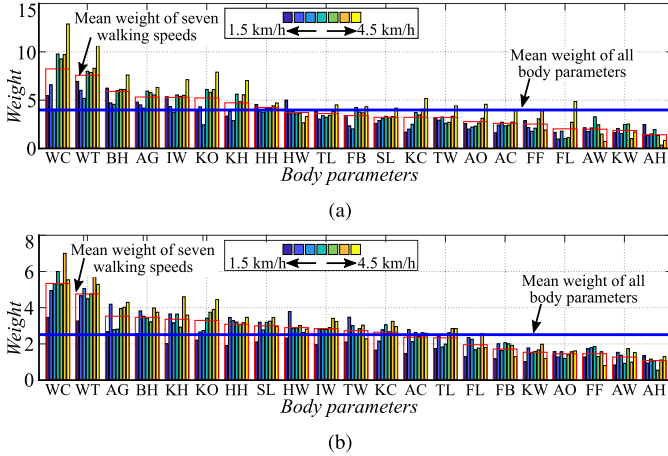
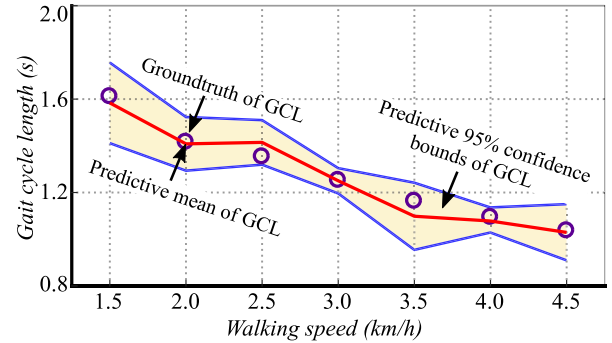


Fig. 9. Weight distribution of each body parameter on gait features at different WSs. (a) Affected weights of gait related body parameters on GCL feature. (b) Affected weights of gait related body parameters on GST features.

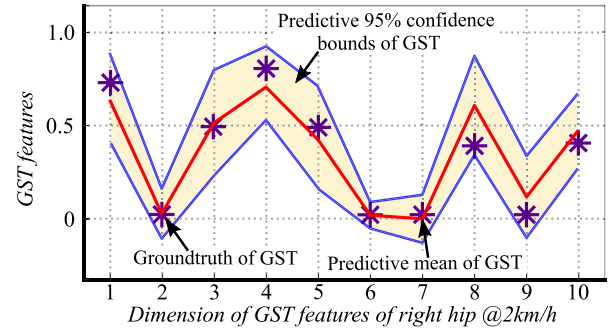
for the same subject and same speed; accordingly, they are very similar. Five sets of features are extracted from five gait cycles, and the averaged gait features can be obtained by averaging them. The joint sequence is reconstructed based on the averaged features, and the results are shown in Fig. 8. The reconstructed joint sequence is basically at the middle of five original gait cycles. This demonstrates that the AENN can extract feasible gait features which are used for regression and reconstruction.

E. Weights of Body Parameters on Gait Pattern

It has been shown that gait pattern is related to many physical parameters. However, it is difficult to determine how much each body parameter affects gait pattern. In this paper, the GPR with ARD is adopted to establish the body parameters and gait features, which can automatically give the affected weights of each body parameters. Fig. 9 shows the affected weights distribution of each body parameter on gait features at different WSs. Among the 21 body parameters, the five most important body parameters that affect the GCL of gait pattern are WC, WT, BH, AG, and IW; the five weakest parameters are AH, KW, AW, FL, and FF. Approximately, the five most important body parameters that affecting the GST features are WC, WT, AG, BH, and KH; the five weakest parameters are AH, AW, FF, AO, and KW.



(a)



(b)

Fig. 10. Predictive gait features based on body parameters and target WS. (a) Predictive GCL feature of one subject during different WSs. (b) Predictive GST features of right hip joint of one subject at a speed of 2 km/h.

F. Prediction of GCL and GST Features

According to Section IV-C, the GPR with ARD is adopted to predict gait features based on the gait subset of the target WS and body parameters. This method can give the predictive mean and confidence bounds. Fig. 10 shows the predictive GCL for one of subjects at different WSs. It can be seen that the predictive means are essentially near the groundtruths, and the 95% of confidence bounds contains all the groundtruths. In terms of GST features prediction, Fig. 10 presents the predictive results of 10-D GST features of the right hip for one of the subjects at a speed of 2 km/h. To sum up, GCL and GST features are the two main types of gait features and GPR can predict them well.

Based on predictive gait features, the gait pattern is reconstructed with the AENN and scaling process, and the result is shown in Fig. 11. Among these lines, the blue lines are the real right hip trajectories of one of the subjects, and the red line is the predicted trajectory of the right hip. It is clear that the predicted trajectory is very close to the real trajectories. Since this is the only one of subjects in Section V-G, a statistical analysis for the model will be presented.

G. Gait Pattern Prediction Analysis

In Section IV-D, the evaluation criteria of the model have been established, including a two-step evaluation. The single-subject experiment has been carried out but not convincing. This section provides a statistical analysis of the model's performance.

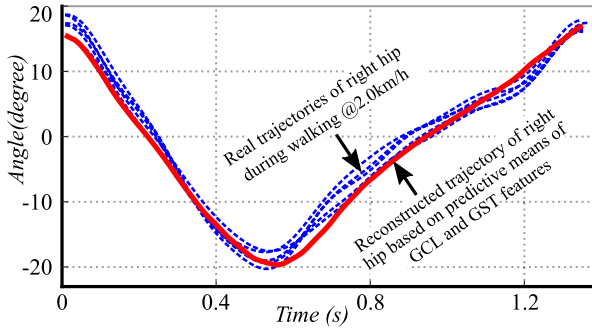


Fig. 11. Real trajectories and the reconstructed trajectory of right hip based on predictive means of GCL and GST features.

TABLE III
DE OF THE PREDICTIVE GCL FEATURE FOR FIVE SUBJECTS AT DIFFERENT WSS

WS	MDE	#A δ_{DE}	#B δ_{DE}	#C δ_{DE}	#D δ_{DE}	#E δ_{DE}
1.5km/h	5.23%	2.68%	3.35%	4.31%	1.12%	0.56%
2.0km/h	5.04%	0.75%	1.99%	2.80%	2.22%	1.07%
2.5km/h	3.78%	4.55%	4.92%	0.90%	4.10%	1.78%
3.0km/h	3.14%	<u>3.81%</u>	2.10%	1.93%	0.64%	1.32%
3.5km/h	4.26%	3.08%	0.48%	2.27%	2.04%	2.06%
4.0km/h	2.33%	<u>3.46%</u>	0.68%	<u>2.83%</u>	1.15%	0.59%
4.5km/h	1.98%	1.03%	1.34%	1.02%	1.94%	0.91%

Due to the limited samples and to make full use of them, one subject is selected as the test target at one time with the remaining 32 subjects as training set. Total 5 subjects are randomly selected as the testing set and labeled as #A, #B, #C, #D, and #E.

For each subject's gait data at a single WS, the maximum deviation is taken as the upper bound and the minimum deviation as the lower bound. Since the groundtruth is obtained by $((L_{\max} + L_{\min})/2)$, the upper and lower bounds are symmetrical. The maximum of deviations of one WS is taken as the allowable maximum DE (MDE). Formula (20) defines a dimensionless variable to describe how far the predicted value deviates from the groundtruth, by which each GCL for each subject at the target WS can be calculated. The DEs of five subjects at seven WSs are presented in Table III; the MDE column shows the allowable MDEs for predictions at different WSs, and the underlined deviations are out of the allowable boundaries. It can be seen that subject #A has three times beyond the boundaries, and subject #B, #C, and #D only have one time each. δ_{DE} of subject #E is all within the boundaries. This indicates that the model can correctly predict the GCL feature for the most part. Subject #A has more errors, probably because of inaccurate measurements or too few training samples.

Second, the statistical analysis of the fixed-length reconstructed gait sequence is performed. According to formula (21), the correlation coefficient is used to evaluate the correlation between the predicted and real gait sequences. Table IV gives the correlation coefficients for each joint of five subjects at different WSs, and the means (standard deviations) of correlation coefficients, as well as the results from the (GPPM) [40] and the clinical gait analysis (CGA) [45]

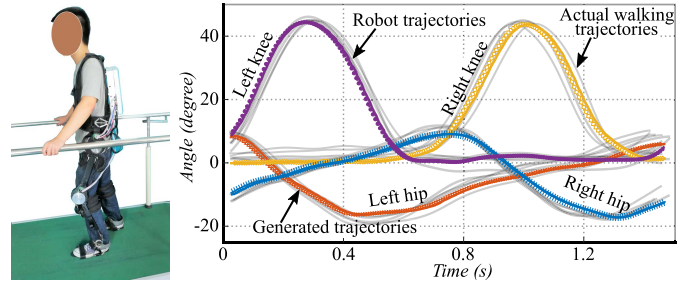


Fig. 12. Subject walks on balance bar with SLEX under the WS of 2 km/h, and the generated trajectories, the SLEX robot's trajectories, and the actual trajectories are shown in the right.

methods. By comparison, the correlation coefficients of the hip and knee obtained by the IGPG method are better than those obtained by the GPPM and CGA methods. The strongest correlation is the right hip joint, where the correlation coefficient reaches 0.99. The standard deviations are also smaller, with a maximum of 0.02. Therefore, from the correlation analysis, the IGPG method gives a better prediction with strong correlation.

The formula (22) defines the MAD to measure the degree of deviation of the predicted gait trajectory from the real trajectory. The MADs of each joint for five subjects at different WSs are presented in Table V. For comparison, the mean and standard deviation for each joint are also given, as well as the mean and standard deviations obtained by the GPPM and CGA methods. It is obvious that the means and standard deviations of MADs obtained by IGPG are both smaller than those obtained by the GPPM and CGA. This also suggests that the trajectory predicted by IGPG is closer to the real trajectory, and the MADs of different subjects have fewer fluctuations.

H. Applying Generated Gait Pattern on SLEX

The final goal of IGPG is the application of the individualized gait pattern on the lower limb exoskeleton robot to help those who are lower limb disabled to walk or to do rehabilitation training with their own gait profile.

From the above-mentioned experiments, the predicted gait patterns for five subjects at different WSs can be obtained. The statistical analysis shows that all subjects have good prediction results except for the GCL feature of #A. Therefore, #B, #C, #D, and #E subjects are selected as the walking subjects wearing SLEX. The SLEX robot works under the predefined trajectory control strategy, the predefined gait trajectory is generated by IGPG. The trajectory tracking is implemented by position-velocity-time (PVT) control algorithm based on C# programming language. The gait data generated offline by the IGPG method are used as the target trajectory, and the SLEX lower limb exoskeleton robot performs its own gait pattern by tracking the target trajectory based on PVT control algorithm.

Then, each subject is asked to walk wearing SLEX on a rehabilitation balance bar, where the subject can maintain their balance by using handrails (see Fig. 12). Fig. 12 only presents an experimental example of one subject walking with SLEX at 2 km/h. The results show that all four subjects complete the walking experiments following the generated gait pattern by

TABLE IV
CORRELATION COEFFICIENTS OF FIVE SUBJECTS OBTAINED BY IGPG AND RESULTS FROM GPPM AND CGA FOR COMPARISON

WS	#A ρ				#B ρ				#C ρ				#D ρ				
	RH	RK	LH	LK													
1.5km/h	0.99	0.98	0.99	0.98	0.99	0.99	0.94	0.98	0.98	0.99	0.99	0.99	0.99	0.99	0.90	0.97	0.96
2.0km/h	0.99	0.98	0.98	0.99	0.99	0.94	0.98	0.96	1.00	0.99	0.94	0.94	0.99	0.95	0.99	0.96	
2.5km/h	0.98	0.97	0.99	0.99	0.99	1.00	0.99	0.99	0.99	0.93	0.99	1.00	1.00	0.95	0.95	0.89	
3.0km/h	0.98	1.00	0.97	0.96	1.00	0.98	0.99	0.99	1.00	0.98	1.00	0.97	0.99	0.95	0.99	0.98	
3.5km/h	0.99	0.99	0.95	0.93	1.00	0.99	0.99	0.99	1.00	0.91	1.00	0.99	1.00	0.96	1.00	0.97	
4.0km/h	0.99	0.98	0.97	0.98	1.00	0.98	0.99	0.99	0.98	0.99	1.00	0.98	1.00	0.99	1.00	0.97	
4.5km/h	0.99	0.98	0.97	0.99	0.99	0.99	0.98	0.99	1.00	0.99	1.00	0.99	0.99	0.98	1.00	0.99	

TABLE IV

(Continued.) CORRELATION COEFFICIENTS OF FIVE SUBJECTS OBTAINED BY IGPG AND RESULTS FROM GPPM AND CGA FOR COMPARISON

WS	#E ρ				IGPG				GPPM [40]		CGA [45]	
	RH	RK	LH	LK	RH	RK	LH	LK	Hip	Knee	Hip	Knee
1.5km/h	0.99	0.98	1.00	0.97								
2.0km/h	0.99	0.99	0.99	0.99								
2.5km/h	0.99	0.99	0.99	0.99	0.99	0.97	0.98	0.98	0.98	0.97	0.87	0.85
3.0km/h	0.98	0.97	1.00	0.99	(0.01)	(0.02)	(0.02)	(0.02)	(0.03)	(0.04)	(0.07)	(0.11)
3.5km/h	0.98	0.99	0.99	1.00								
4.0km/h	0.99	1.00	1.00	1.00								
4.5km/h	0.97	0.99	1.00	0.99								

TABLE V

MADS OF FIVE SUBJECTS OBTAINED BY IGPG AND RESULTS FROM GPPM AND CGA FOR COMPARISON

WS	#A MAD				#B MAD				#C MAD				#D MAD			
	RH	RK	LH	LK												
1.5km/h	3.38	4.27	1.57	3.39	1.62	1.55	2.50	3.14	4.91	2.59	3.34	1.71	1.14	4.97	1.99	3.69
2.0km/h	2.70	2.93	4.92	2.74	1.92	3.90	2.36	2.85	0.39	2.62	3.05	3.70	1.70	3.57	2.00	3.13
2.5km/h	2.67	3.28	3.46	2.76	3.29	3.65	1.00	2.27	2.05	5.58	2.08	2.11	3.27	4.45	2.82	5.73
3.0km/h	4.36	2.84	2.22	5.05	1.93	3.02	2.93	2.53	1.25	4.18	1.12	3.29	5.34	2.86	1.20	4.61
3.5km/h	2.41	3.60	4.21	4.70	1.45	2.27	1.55	2.22	3.47	5.90	4.13	3.97	2.59	4.05	1.36	4.03
4.0km/h	2.58	4.26	2.82	5.23	2.76	2.97	1.31	5.02	4.77	4.79	3.89	9.77	2.27	1.85	4.37	5.03
4.5km/h	2.34	2.82	2.93	2.68	2.79	3.46	2.41	3.20	4.85	4.56	2.76	5.42	2.79	2.63	1.93	6.09

TABLE V

(Continued.) MADS OF FIVE SUBJECTS OBTAINED BY IGPG AND RESULTS FROM GPPM AND CGA FOR COMPARISON

WS	#E MAD				IGPG				GPPM [40]		CGA [45]	
	RH	RK	LH	LK	RH	RK	LH	LK	Hip	Knee	Hip	Knee
1.5km/h	2.06	1.92	3.22	2.18								
2.0km/h	1.47	2.90	2.12	2.31								
2.5km/h	1.08	2.04	2.95	3.66	2.60	3.40	2.62	3.64	3.73	5.41	7.66	9.28
3.0km/h	3.07	5.07	4.01	3.80	(1.18)	(1.11)	(1.03)	(1.64)	(1.64)	(2.01)	(1.78)	(3.07)
3.5km/h	1.84	1.75	3.14	1.38								
4.0km/h	1.58	2.48	2.98	2.04								
4.5km/h	2.89	3.35	1.13	1.85								

IGPG, and they express that the individualized gait patterns are consistent with their walking habits.

VI. CONCLUSION

With the development of sharing technology, it is possible for the expensive exoskeleton robot to be widely used. However, due to the uniqueness of gait pattern, little research on how to generate suitable gait pattern of lower limb exoskeleton robot for the wearer's own physical characteristics is involved. To this end, lots of gait data and body parameters are collected. First, the gait sequence is parameterized to extract the gait features. Then, the GPR with ARD was adopted to establish

the mapping relationships between the body parameters and the gait features at different WSs and to predict the suitable gait features according to given body parameters and target WS. Finally, the individualized gait pattern was reconstructed based on the predicted gait features. The experimental results demonstrated that the IGPG can better predict the gait pattern of unknown subject at a target WS and the feasibility of applying the predicted gait pattern on SLEX robot. Meanwhile, the IGPG can also give the affected weights of different body parameters on gait pattern, which provided a reference for optimizing the lower limb exoskeleton robot in the future.

However, due to the small data set, some weights of body parameters may be deviated. Predictably, with the expansion of data set, the more important or the weaker body parameters affecting gait pattern will become clearer. When it comes to sharing application, the training set can be increased continuously with the help of sharing technology, and the prediction accuracy of individualized gait pattern will be improved.

ACKNOWLEDGMENT

The authors would like to thank all subjects who participated in experiments and the members of SIAT exoskeleton team.

REFERENCES

- [1] C. D. Lim, C.-M. Wang, C.-Y. Cheng, Y. Chao, S.-H. Tseng, and L.-C. Fu, "Sensory cues guided rehabilitation robotic walker realized by depth image-based gait analysis," *IEEE Trans. Autom. Sci. Eng.*, vol. 13, no. 1, pp. 171–180, Jan. 2016.
- [2] S. Maggioni *et al.*, "Robot-aided assessment of lower extremity functions: A review," *J. Neuroeng. Rehabil.*, vol. 13, no. 1, p. 72, 2016.
- [3] J. Meuleman, E. van Asseldonk, G. van Oort, H. Rietman, and H. van der Kooij, "LOPES II—Design and evaluation of an admittance controlled gait training robot with shadow-leg approach," *IEEE Trans. Neural Syst. Rehabil. Eng.*, vol. 24, no. 3, pp. 352–363, Mar. 2016.
- [4] A. Domingo and T. Lam, "Reliability and validity of using the Lokomat to assess lower limb joint position sense in people with incomplete spinal cord injury," *J. Neuroeng. Rehabil.*, vol. 11, no. 1, p. 167, 2014.
- [5] S. K. Banala, S. H. Kim, S. K. Agrawal, and J. P. Scholz, "Robot assisted gait training with active leg exoskeleton (ALEX)," *IEEE Trans. Neural Syst. Rehabil. Eng.*, vol. 17, no. 1, pp. 2–8, Feb. 2009.
- [6] S. Wang *et al.*, "Design and control of the MINDWALKER exoskeleton," *IEEE Trans. Neural Syst. Rehabil. Eng.*, vol. 23, no. 2, pp. 277–286, Mar. 2015.
- [7] H. Wang, C. Wang, W. Chen, X. Liang, and Y. Liu, "Three-dimensional dynamics for cable-driven soft manipulator," *IEEE/ASME Trans. Mechatronics*, vol. 22, no. 1, pp. 18–28, Feb. 2017.
- [8] A. Kozlowski, T. Bryce, and M. Dijkers, "Time and effort required by persons with spinal cord injury to learn to use a powered exoskeleton for assisted walking," *Topics Spinal Cord Injury Rehabil.*, vol. 21, no. 5, pp. 110–121, 2015.
- [9] A. Esquenazi, M. Talaty, A. Packel, and M. Saulino, "The ReWalk powered exoskeleton to restore ambulatory function to individuals with thoracic-level motor-complete spinal cord injury," *Amer. J. Phys. Med. Rehabil.*, vol. 91, no. 11, pp. 911–921, 2012.
- [10] A. Tsukahara, Y. Hasegawa, K. Eguchi, and Y. Sankai, "Restoration of gait for spinal cord injury patients using HAL with intention estimator for preferable swing speed," *IEEE Trans. Neural Syst. Rehabil. Eng.*, vol. 23, no. 2, pp. 308–318, Mar. 2015.
- [11] C. Hartigan *et al.*, "Mobility outcomes following five training sessions with a powered exoskeleton," *Topics Spinal Cord Injury Rehabil.*, vol. 21, no. 2, pp. 93–99, 2015.
- [12] G. Barbareschi, R. Richards, M. Thornton, T. Carlson, and C. Holloway, "Statically vs dynamically balanced gait: Analysis of a robotic exoskeleton compared with a human," in *Proc. 37th Annu. Int. Conf. IEEE Eng. Med. Biol. Soc. (EMBC)*, Aug. 2015, pp. 6728–6731.
- [13] X. Hu *et al.*, "Emotion-aware cognitive system in multi-channel cognitive radio ad hoc networks," *IEEE Commun. Mag.*, vol. 56, no. 4, pp. 180–187, Apr. 2018.
- [14] J. Zhang *et al.*, "Energy-latency trade-off for energy-aware offloading in mobile edge computing networks," *IEEE Internet Things J.*, to be published, doi: [10.1109/JIOT.2017.2786343](https://doi.org/10.1109/JIOT.2017.2786343).
- [15] C. J. Martin, "The sharing economy: A pathway to sustainability or a nightmarish form of neoliberal capitalism?" *Ecol. Econ.*, vol. 121, pp. 149–159, Jan. 2016.
- [16] B. Cohen and J. Kietzmann, "Ride on! Mobility business models for the sharing economy," *Org. Environ.*, vol. 27, no. 3, pp. 279–296, 2014.
- [17] X. Hu, X. Li, E. C.-H. Ngai, V. C. M. Leung, and P. Kruchten, "Multidimensional context-aware social network architecture for mobile crowdsensing," *IEEE Commun. Mag.*, vol. 52, no. 6, pp. 78–87, Jun. 2014.
- [18] Z. Ning *et al.*, "A cooperative quality-aware service access system for social Internet of vehicles," *IEEE Internet Things J.*, to be published, doi: [10.1109/JIOT.2017.2764259](https://doi.org/10.1109/JIOT.2017.2764259).
- [19] A. M. Dollar and H. Herr, "Lower extremity exoskeletons and active orthoses: Challenges and state-of-the-art," *IEEE Trans. Robot.*, vol. 24, no. 1, pp. 144–158, Feb. 2008.
- [20] S. W. Lee, T. Yi, J. W. Jung, and Z. Bien, "Design of a gait phase recognition system that can cope with EMG electrode location variation," *IEEE Trans. Autom. Sci. Eng.*, vol. 14, no. 3, pp. 1429–1439, Jul. 2017.
- [21] T. Yan, M. Cempini, C. M. Oddo, and N. Vitiello, "Review of assistive strategies in powered lower-limb orthoses and exoskeletons," *Robot. Auto. Syst.*, vol. 64, pp. 120–136, Feb. 2015.
- [22] B. Xu and F. Sun, "Composite intelligent learning control of strict-feedback systems with disturbance," *IEEE Trans. Cybern.*, vol. 48, no. 2, pp. 730–741, Feb. 2018.
- [23] A. Kale *et al.*, "Identification of humans using gait," *IEEE Trans. Image Process.*, vol. 13, no. 9, pp. 1163–1173, Sep. 2004.
- [24] M. H. Schwartz, A. Rozumalski, and J. P. Trost, "The effect of walking speed on the gait of typically developing children," *J. Biomech.*, vol. 41, no. 8, pp. 1639–1650, 2008.
- [25] Y. Blanc, C. Balmer, T. Landis, and F. Vingerhoets, "Temporal parameters and patterns of the foot roll over during walking: Normative data for healthy adults," *Gait Posture*, vol. 10, no. 2, pp. 97–108, 1999.
- [26] L. Wang, T. Tan, H. Ning, and W. Hu, "Silhouette analysis-based gait recognition for human identification," *IEEE Trans. Pattern Anal. Mach. Intell.*, vol. 25, no. 12, pp. 1505–1518, Dec. 2003.
- [27] G. E. Hinton and R. R. Salakhutdinov, "Reducing the dimensionality of data with neural networks," *Science*, vol. 313, no. 5786, pp. 504–507, 2006.
- [28] R. M. Neal, *Bayesian Learning for Neural Networks* (Lecture Notes in Statistics), vol. 118. New York, NY, USA: Springer-Verlag, 1996.
- [29] H. Zhu, M. Hou, C. Wang, and M. Zhou, "An efficient outpatient scheduling approach," *IEEE Trans. Autom. Sci. Eng.*, vol. 9, no. 4, pp. 701–709, Oct. 2012.
- [30] H. Kim, H. Song, S. Lee, H. Kim, and I. Song, "A simple approach to share users' own healthcare data with a mobile phone," in *Proc. 8th Int. Conf. Ubiquitous Future Netw.*, Jul. 2016, pp. 453–455.
- [31] X. H. Chen, Y. L. Ma, G. F. Zhang, and B. Liu, "Cloud computing-based rehabilitation services information system," *Appl. Mech. Mater.*, vol. 415, pp. 389–395, Sep. 2013.
- [32] D. Sanz-Merodio, M. Cestari, J. C. Arevalo, and E. Garcia, "Control motion approach of a lower limb orthosis to reduce energy consumption," *Int. J. Adv. Robot. Syst.*, vol. 9, no. 6, p. 232, 2012.
- [33] K. Suzuki, G. Mito, H. Kawamoto, Y. Hasegawa, and Y. Sankai, "Intention-based walking support for paraplegia patients with Robot Suit HAL," *Adv. Robot.*, vol. 21, no. 12, pp. 1441–1469, 2007.
- [34] H. Vallery, E. H. F. van Asseldonk, M. Buss, and H. van der Kooij, "Reference trajectory generation for rehabilitation robots: Complementary limb motion estimation," *IEEE Trans. Neural Syst. Rehabil. Eng.*, vol. 17, no. 1, pp. 23–30, Feb. 2009.
- [35] T. Kagawa, H. Ishikawa, T. Kato, C. Sung, and Y. Uno, "Optimization-based motion planning in joint space for walking assistance with wearable robot," *IEEE Trans. Robot.*, vol. 31, no. 2, pp. 415–424, Apr. 2015.
- [36] K. K. Karunakaran, K. M. Abbruzzese, H. Xu, and R. A. Foulds, "The importance of haptics in generating exoskeleton gait trajectory using alternate motor inputs," *IEEE Trans. Neural Syst. Rehabil. Eng.*, vol. 25, no. 12, pp. 2328–2335, Dec. 2017.
- [37] J. Zhang *et al.*, "Human-in-the-loop optimization of exoskeleton assistance during walking," *Science*, vol. 356, no. 6344, pp. 1280–1284, Jun. 2017.
- [38] H. B. Lim, P. L. Trieu, K. H. Hoon, and K. H. Low, "Natural gait parameters prediction for gait rehabilitation via artificial neural network," in *Proc. IEEE Int. Conf. Intell. Robots Syst. (IROS)*, Taipei, Taiwan, Oct. 2010, pp. 5398–5403.
- [39] P. Wang, K. H. Low, and A. H. McGregor, "A subject-based motion generation model with adjustable walking pattern for a gait robotic trainer: NaTure-gaits," in *Proc. IEEE Int. Conf. Intell. Robots Syst. (IROS)*, San Francisco, CA, USA, Sep. 2011, pp. 1743–1748.
- [40] T. P. Luu, K. H. Low, X. Qu, H. B. Lim, and K. H. Hoon, "An individual-specific gait pattern prediction model based on generalized regression neural networks," *Gait Posture*, vol. 39, no. 1, pp. 443–448, 2014.

- [41] Y. Yun, H.-C. Kim, S. Y. Shin, J. Lee, A. D. Deshpande, and C. Kim, "Statistical method for prediction of gait kinematics with Gaussian process regression," *J. Biomech.*, vol. 47, no. 1, pp. 186–192, Jan. 2014.
- [42] W. Wu, D. Wang, T. Wang, and M. Liu, "A personalized limb rehabilitation training system for stroke patients," in *Proc. IEEE Int. Conf. Robot. Biomimetics*, Qingdao, China, Dec. 2016, pp. 1924–1929.
- [43] D.-X. Liu, X. Wu, W. Du, C. Wang, C. Chen, and T. Xu, "Deep spatial-temporal model for rehabilitation gait: Optimal trajectory generation for knee joint of lower-limb exoskeleton," *Assem. Autom.*, vol. 37, no. 3, pp. 369–378, 2017.
- [44] C. E. Rasmussen and C. K. I. Williams, *Gaussian Processes for Machine Learning*. Cambridge, MA, USA: MIT Press, 2006.
- [45] E. K. Antonsson and R. W. Mann, "The frequency content of gait," *J. Biomech.*, vol. 18, no. 1, pp. 39–47, 1985.



Xinyu Wu (M'13) received the B.E. and M.E. degrees from the Department of Automation, University of Science and Technology of China, Hefei, China, in 2001 and 2004, respectively, and the Ph.D. degree from the Chinese University of Hong Kong, Hong Kong, in 2008.

He is currently a Professor with the Shenzhen Institutes of Advanced Technology, Chinese Academy of Sciences, Shenzhen, China, where he is the Director of the Center for Intelligent Bionic. He has authored or co-authored over 180 papers and two

monographs. His research interests include computer vision, robotics, and intelligent system.



Du-Xin Liu (S'17) received the B.Sc. degree in electronic and information engineering from the Qilu University of Technology, Jinan, China, in 2011, and the M.Sc. degree in electronic science and technology from the University of Science and Technology Beijing, Beijing, China, in 2014. He is currently pursuing the Ph.D. degree in pattern recognition and intelligent systems with the University of Chinese Academy of Sciences, Beijing.

His current research interests include wearable exoskeleton robot and intelligent robot system.



Ming Liu (M'12) received the B.A. degree in automation from Tongji University, Shanghai, China, in 2005, and the Ph.D. degree from the Department of Mechanical and Process Engineering, ETH Zürich, Zürich, Switzerland, in 2013.

He was a Master Visiting Scholar with Erlangen–Nuremberg University, Erlangen, Germany, and the Fraunhofer Institute IISB, Erlangen. He is currently with the Department of Electronics and Communication Engineering, Department of Computer Science, and Robotics Institute, Hong Kong University of

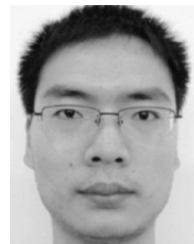
Science and Technology, Hong Kong. His research interests include dynamic environment modeling, deep learning for robotics, 3-D mapping, machine learning, and visual control.

Dr. Liu was a recipient of the Best Student Paper Award at the IEEE MFI 2012, the Best Paper in Information Award at the IEEE ICIA 2013, the Best RoboCup Paper at the IEEE IROS 2013, and twice the Winning Prize of the Chunhui-Cup Innovation Contest.



Chunjie Chen received the B.Sc. and M.Sc. degrees from Wuhan University, Wuhan, China, in 2005 and 2007, respectively. He is currently pursuing the Ph.D. degree with the Chinese Academy of Sciences, Shenzhen, China.

His research interests include exoskeleton robot, service robots, and intelligent system.



Huiwen Guo received the M.E. degree in control science and engineering from Hunan University, Changsha, China, in 2013, and the Ph.D. degree in pattern recognition and intelligent system from the University of Chinese Academy of Sciences, Beijing, China, in 2017.

He is currently a Post-Doctor Scholar with the Shenzhen Institutes of Advanced Technology, Chinese Academy of Sciences, Shenzhen, China. His research interests include computer vision and robot vision.